

ILLUMINATED, AND ENLIGHTENED, BY GRB 991216

M. VIETRI

Universit  di Roma 3, Via della Vasca Navale 84, I-00147 Roma, Italy; e-mail: vietri@fis.uniroma3.it

G. GHISELLINI AND D. LAZZATI¹

Osservatorio Astronomico di Brera, Via E. Bianchi 46 I-23807 Merate, Italy; e-mail: gabriele@merate.mi.astro.it

F. FIORE AND L. STELLA

Osservatorio Astronomico di Roma, Via Frascati 33, I-00040 Monteporzio Catone, Italy; e-mail: fiore,stella@coma.mporzio.astro.it

Accepted for publication in *ApJ Letters*

ABSTRACT

We consider models for the generation of the emission line recently discovered in the X-ray afterglow spectrum of several bursts, and especially of GRB 991216 observed by *Chandra*. These observations suggest the presence of 0.1–1 solar masses of iron in the vicinity of the bursts. We show that there are strong geometrical and kinematical constraints on the line emitting material. We discuss several classes of models, favoring one where the line photons are produced by reflection off the walls of a wide funnel of semi-opening angle $\vartheta \approx 45^\circ$ excavated in a young (a few months old) supernova remnant made of $\approx 10M_\odot$ with radius 6×10^{15} cm, and $\approx 1M_\odot$ of iron, providing strong support for the SupraNova model.

Subject headings: gamma rays: bursts — radiation mechanisms: nonthermal — line: formation

1. INTRODUCTION

There are now five bursts displaying evidence for large amounts of X-ray line emitting material around the site of the explosion: four (GRB 970508, Piro et al., 1999; GRB 970828, Yoshida et al., 1999; GRB 991216, Piro et al., 2000, hereafter P2000; GRB 000214, Antonelli et al., 2000) show an emission feature during the afterglow, and one (GRB 990705, Amati et al., 2000) displays an edge in absorption during the burst itself. Though most of these observations, carried out with three different instruments (*BeppoSAX*, *ASCA*, *Chandra*) may perhaps be seen as only marginally significant, at least one of them (GRB 991216, observed with *Chandra*) shows a 3.49 ± 0.06 keV line significant at a $\sim 4\sigma$ level. If the line is identified with the recombination $K\alpha$ line from H-like iron (6.97 keV), the inferred redshift is $z = 1.00 \pm 0.02$ consistent with the largest redshift system ($z = 1.02$) seen in absorption in the optical (Vreeswijk et al., 2000). The line is also resolved by *Chandra*, displaying a width corresponding to $0.05c$ (P2000). These observations started 37 hr after the burst, and lasted for about 3 hr. The line and the 2–10 keV continuum fluxes were $\sim 1.6 \times 10^{-13}$ and $\sim 2.4 \times 10^{-12}$ erg s⁻¹ cm⁻², respectively. At a redshift $z = 1.02$ this implies an emission rate of iron line photons of $\dot{N}_{\text{line}} \simeq 4 \times 10^{52}$ s⁻¹, luminosity $L_{\text{line}} \simeq 4 \times 10^{44}$ erg s⁻¹ and total energy $E_{\text{line}} \sim 3 \times 10^{49}$ erg (assuming steady emission for $40/(1+z)$ hr, with $H_0 = 75$ km s⁻¹ Mpc⁻¹ and $q_0 = 0.5$). If each iron atom produces k line photons, the required iron mass is $M_{\text{Fe}} \simeq 195 k^{-1} M_\odot$. Bringing this mass down to $\sim 0.1 M_\odot$ implies $k > 2000$ which in turn implies a limit on the recombination time². This translates into the condition that the electron density is $n_e > 10^{10} T_7^{3/4}$ cm⁻³; the high electron temperature $T = 10^7 T_7$ K comes from interpreting the broad bump that was marginally detected with *Chandra* at an energy of 4.4 ± 0.5 keV in terms of the recombination continuum of H-like iron (9.28 keV). As discussed for GRB 950708 (Lazzati et al. 1999), the detection of the line implies the presence of a sizable fraction

of solar mass of pure iron concentrated in the vicinity of the burster. This is naturally accounted for in the SupraNova scenario (Vietri & Stella 1998), where the burst follows with few months (to several years) delay a supernova explosion. Alternative explanations invoke extremely iron enriched massive winds (see Weth et al. 2000) to produce the observed line.

Observation of the line t_{obs} after the burst implies that the line emitting material must be within $\sim ct_{\text{obs}}/(1+z)$ from the burst site: this region must then be *compact*, contain $\sim 0.1 M_\odot$ only in iron, but nevertheless be optically thin to electron scattering, such that Comptonization does not broaden the line beyond the observed width. We call this the *size problem*.

Furthermore, if we interpret the line width as due to the velocity of a supernova remnant, the limit on the size allows to estimate the age of the remnant which for GRB 991216 turns out to be ~ 15 days. At this time (see Fig. 1), cobalt nuclei would outnumber nickel and iron nuclei and the line would be produced mainly by cobalt, not iron, at an energy $\epsilon = 7.5/(1+z)$ keV. We call this the *kinematic problem*.

We discuss in section 2 the constraints implied by the line observation; we then present in section 3 three scenarios which could produce the observed line. Two of them are found to be viable only by adopting ad hoc assumptions or through fine tuning, while a third scenario, the “wide funnel” scenario, appears to be more promising. In section 4 we discuss our results.

2. PHYSICAL AND GEOMETRICAL CONDITIONS

The detection of emission features in the afterglow spectra of GRBs some hours after the GRB event poses a strong constraint on the location of the line emitting material. If the line is detected after t_{obs} from the burst explosion the material must be located within a distance R given by

$$R \leq \frac{ct_{\text{obs}}}{1+z} \frac{1}{1-\cos\vartheta} \simeq \frac{1.1 \times 10^{15}}{1+z} \frac{t_{\text{obs}}}{10\text{h}} \frac{1}{1-\cos\vartheta} \text{ cm}, \quad (1)$$

¹Present address: Institute of Astronomy, Madingley Road, Cambridge CB3 0HA, UK; e-mail: lazzati@ast.cam.ac.uk

²From the formulae given in Verner & Ferland (1996), the recombination time can be approximated by $t_{\text{rec}} \sim 12.7 T_7^{3/4} n_{10}^{-1}$ s in the temperature range $10^6 < T < 10^8$ K.

where ϑ is the angle between the line emitting material and the line of sight at the GRB site.

This limit has very important implications, because:

i) the scattering optical depth is large:

$$\tau_T = \frac{\sigma_T M}{4\pi R^2 \mu m_p} \geq 54 \frac{(M/M_\odot)(1+z)^2(1-\cos\vartheta)^2}{\mu(t_{\text{obs}}/10\text{h})^2} , \quad (2)$$

where $\mu = 1, 1.2$ and 2 for pure hydrogen, solar composition, and no hydrogen, respectively.

ii) For a radial velocity of the remnant of $v = 10^9 v_9 \text{ cm s}^{-1}$ the time elapsed from the SN is $t_{\text{SN}} \simeq 12.5(t_{\text{obs}}/10\text{hr})/[(1+z)(1-\cos\vartheta)v_9]$ days. Such short times implies that most of the ^{56}Co nuclei (and a fraction of the ^{56}Ni nuclei) have not yet decayed to ^{56}Fe (half-life of 77.3 and 6.08 days, respectively). In Fig. 1 we show the normalized abundances of the nickel, cobalt and iron as a function of time elapsed from the SN explosion.

In order to produce the line by frequent recombinations and ionizations, a sufficiently high ionizing flux is required, together with a large number of H-like iron ions, FeXXVI. An efficient use of these ions demands that τ_{FeXXVI} , the photoionization optical depth for FeXXVI, is close to or larger than unity. With a photoionization cross section of $\sigma_{\text{FeXXVI}} \sim 1.2 \times 10^{-20} \text{ cm}^{-2}$, and abundance ratio of $\xi = M_{\text{FeXXVI}}/M_{\text{Fe}}$, we have

$$\tau_{\text{FeXXVI}} = \frac{\sigma_{\text{FeXXVI}} \xi M_{\text{Fe}}}{56m_p 4\pi R^2} = 2 \times 10^3 \frac{\xi}{R_{15}^2} \frac{M_{\text{Fe}}}{0.1 M_\odot} . \quad (3)$$

A strict *lower* limit on the power of the ionizing continuum comes from the line flux itself. For GRB 991216, assuming an illumination time equal to 20 hr, we require $E_{\text{ion}} > 3 \times 10^{49} \text{ erg}$. In GRB 991216 there is no hint of *rebursting* in the X-ray afterglow (which instead was observed in GRB 970508). Even in the case of an illuminating continuum not directly visible by us, we require that the scattered flux produced by the line emitting material does not affect the afterglow emission, i.e. it must contribute less than $10^{-12} \text{ erg cm}^{-2} \text{ s}^{-1}$ to the observed flux. This gives the *upper* limit $\min(1, \tau_T) E_{\text{ion}} < 1.8 \times 10^{50} \text{ erg}$.

2.1. Compton broadening and Thomson optical depth

If the emitting atoms are diluted in an electron cloud, then simple radiative transfer yields a fraction of unscattered flux equal to $[1 - \exp(-\tau_T)]/\tau_T$, while if the scattering cloud surrounds a central source the fraction becomes $\exp(-\tau_T)$. If the scattering electrons have a temperature in the $\sim 10^7 \text{ K}$ range (according to the indication that the recombination continuum observed in GRB991216 might be broad, see P2000), the average energy shift of line photons that are scattered only once is $\Delta E/E \approx 0.063(kT/1\text{keV})$ (Pozdnyakov, Sobol & Sunyaev 1983). *This is already broader than the observed line width.* Multiple scatterings would broaden the line even further, making this increasingly difficult to detect against the X-ray continuum. If the line detected by P2000 were made up by those line photons that escape unscattered from a medium with $\tau_T > 1$, then the problem with the line flux would be exacerbated and a factor of τ_T higher mass in iron required.

An alternative possibility is that the electron temperature is substantially lower than 10^7 K , say $\sim 10^6 \text{ K}$, as might be expected if the ionizing continuum were steep and extended to sufficiently low energies. In particular, there might exist a suitable combination of τ_T and temperature such that Compton broadening explains the observed line width. In this case,

however, the centroid of the line would be somewhat redshifted (line photons are mostly backscattered by the colder electrons) and the recombination continuum narrower. Owing to the poor statistics, the recombination continuum of GRB 991216 does not allow a firm constraint to be placed on the electron temperature. Yet, the models we examine in Section 3 are largely independent of the presence of the recombination emission continuum and its width.

3. THE MODELS

We can roughly divide the models into *transmission* and *reflection* models. If we see the line in reflection, line photons come from the layer with $\tau_{\text{FeXXVI}} = \text{several}^3$. For an iron abundance greater than the solar value, in this layer $\tau_T \leq 1$. In general, transmission models require $\tau_T < 1$ and $\tau_{\text{FeXXVI}} \sim 1$, while reflection models require $\tau_{\text{FeXXVI}} > \tau_T$. Each iron atom must produce ~ 2000 iron photons, and this requires an electron density larger than 10^{10} cm^{-3} .

The large equivalent widths inferred from the X-ray line features in GRB 991216 ($EW = 0.5 \text{ keV}$) and, especially, GRB 970508 ($EW \sim 1 \text{ keV}$), GRB 970828 ($EW \sim 3 \text{ keV}$) and GRB 000214 ($EW \sim 2 \text{ keV}$) favor models in which the line originates in reflection, not transmission. In reflection, in fact, the ionizing flux is always efficiently reprocessed in line photons in the $\tau_{\text{Fe}} \sim 1$ layer, while in transmission this happens only for a particular tuning of the FeXXVI and the free electron densities.

The three alternative geometries considered, all producing lines in reflection, are sketched in Fig. 2 and described below.

In reflection models, we can derive the photon line luminosity by estimating the volume V_{em} effectively contributing to the line emission, and assuming a given iron mass. If the layer contributing to the emission has $\tau_T \sim 1$ (in order to avoid excessive Compton broadening of the line), and in this layer $\tau_{\text{FeXXVI}} \sim a$ few (to efficiently absorb the continuum), we have $V_{\text{em}} = S/(\sigma_T n_e)$, where S is the emitting surface. The line emission rate from V_{em} is then

$$\dot{N}_{\text{Fe}} = \frac{N_{\text{Fe}}}{t_{\text{rec}}} = \frac{S n_{\text{Fe}}}{1.3 \times 10^{11} T_7^{3/4} \sigma_T} \sim 3 \times 10^{53} \frac{(M_{\text{Fe}}/M_\odot)}{T_7^{3/4} \Delta R_{15}} \text{ s}^{-1} . \quad (4)$$

where we have assumed that the *total* volume is $V = S\Delta R$ (slab or shell geometry). Eq. 4 shows that the total iron mass must be a sizable fraction of a solar mass to obtain the observed line flux ($4 \times 10^{52} \text{ s}^{-1}$), within the range provided by the largest values observed so far, $0.9M_\odot$ for both Type Ic (SN 1998bw, Sollerman et al., 2000), and Type Ia (SN1991T, Filippenko et al., 1992). But notice also that Eq. 4 all by itself establishes that the line emitting material must be a SNR: no other known astrophysical object contains so much iron, not even the largest known stars (though these fail by a factor of a few only).

Eq. 4 has another important implication. It fixes M/R , and since R is fixed (for a given geometry, see below) by the time-delay constraint, it follows that the cloud density is also fixed, to within an order of magnitude. Solutions with densities much exceeding (or much below) $\approx 10^{10} \text{ cm}^{-3}$ are excluded.

3.1. The wide funnel

If the GRB explodes within the young remnant of a supernova, we must consider two possibilities: a plerionic and a shell

³What we call FeXXVI might well be CoXXVII or NiXXVIII, see section 2.

remnant. In the first case, we consider a wide funnel excavated in a young plerionic remnant. This can solve the *size problem*, since it extends to large radii but, at the same time (Eq. 1), can maintain the time–delay contained because it is naturally built close to the polar axis (assumed to be close to the line of sight). The geometrical set–up is sketched in the left panel of Fig. 2. Fixing the line photons rate (Eq. 4) yields $R = 6 \times 10^{15}$ cm, and thus an opening angle $\vartheta = 48^\circ$, to fit the time–delay. For any reasonable SN composition, these parameters imply $n_e > 10^{10}$ cm $^{-3}$. The funnel walls are probably not straight (like in a cone geometry), but curved instead, like the surface of the coffee in a cup when it is spun up, and can then be efficiently illuminated by the ionizing flux coming from a central source. Assuming a cone geometry for simplicity, we can rewrite Equation 4 as

$$\dot{N}_{\text{Fe}} = 3.3 \times 10^{52} \frac{(M_{\text{Fe}}/M_{\odot})}{T_7^{3/4} (R_{15}/6)} \tan \vartheta \text{ s}^{-1}. \quad (5)$$

where in this case R (the radius of the filled remnant) has been used instead of ΔR and $\tan \vartheta$ takes into account the geometry of the funnel. This is a lower limit, since a parabolic geometry has a larger funnel surface and we neglected the (likely) density stratification inside the remnant.

We consider now the kinematic properties of the funnel. Since the funnel’s normal is *not* parallel to the incident photon’s momentum, we expect radiation pressure to exert a force parallel to the surface accelerating the layer $\tau_T = 1$ because this reflects isotropically photons arriving from a specific direction. Calling φ the angle between the funnel’s local outward normal and the incident photon’s arrival direction we thus expect the absorbed fluence E_{ion} to accelerate the funnel layer to a speed $v_f = \sin \varphi (2E_{\text{ion}}/M_{\text{layer}})^{1/2} \simeq 10^4 E_{\text{ion},50}^{1/2} \sin \varphi \text{ km s}^{-1}$ for an external radius $R = 6 \times 10^{15}$ cm. Thus, we expect ablation by radiation pressure to be able to propel the reflecting layer to the velocities comparable to those seen in GRB991216 by P2000.

The funnel model can thus explain the observed line broadening even in a relatively old SNR. If we consider a remnant ejected with $v_{\text{ej}} = 3000 \text{ km s}^{-1}$, a typical value for type II SNe, we obtain a remnant age of $t_{\text{SNR}} \sim 230$ days, enough to turn most of the ^{56}Ni and ^{56}Co nuclei into ^{56}Fe nuclei (see Fig. 1). The emitting iron is then boosted to higher velocity when illuminated by the ionizing flux, thus circumventing the kinematical problem.

3.2. Back of the remnant

Let us now consider a shell remnant. We assume that the remnant is characterized by a wide opening, such that a substantial fraction of the inner face of the remnant is visible (central panel of Fig. 2). This is possibly illuminated by the photons of the burst and its afterglow and, more likely, by the shock produced by the impact of the fireball (Böttcher 2000). Line photons are produced in the layer with $\tau_{FeXXVI} \sim \text{few}$. As in the previous model, the remnant could have been ‘slowly’ expanding until it is accelerated by the burst photons. As we see the internal part of the remnant, the *size* limit discussed in Section 2 is tighter, and we detect mainly redshifted photons. With a remnant distance of $R = 10^{15}$ cm and velocity of 5,000 km s $^{-1}$ the age turns out to be ~ 20 days; this is close to the peak of ^{56}Co (see Fig. 1). However, the 7.5 keV ^{56}Co line would be observed with a substantial redshift (and therefore mimic a ^{56}Fe 6.97 keV line), if the burst photons increased the expanding velocity to $\sim 20,000 \text{ km s}^{-1}$ (this implies that the burst

emitted a few times 10^{52} erg sideways, for a $10 M_{\odot}$ remnant). In this model the observed line width of 15,000 km s $^{-1}$ would require that only a limited range of projections of the radial expansion velocity vectors are observed. This solution does not appear convincing as it involves a fine tuning between the energy produced sideways and the mass of the remnant, in order to have the correct expansion velocity. It would however naturally explain the different centroid energy of the line observed in GRB 970508: since the line is redshifted by the shell expansion, we expect a distribution of observed energies as a consequence of different velocities of the remnant.

3.3. Back–illuminated equatorial material

The two models discussed above assume that a supernova explosion preceded the GRB by some months. We now explore the possibility of a simultaneous GRB–“supernova” explosion. Consider then a scenario in which the GRB ejects and accelerates a small amount of matter in a collimated cone, while a large amount of matter is instead ejected, at sub–relativistic speeds, along the progenitor’s equator. For illustration, assume equal amounts of energy, 10^{52} erg, in both directions, and $1 M_{\odot}$ expelled along the equator. Then $v_{\text{eq}}/c = 0.148 E_{52}^{1/2} (M/M_{\odot})^{-1/2}$. Massive star progenitors are inevitably surrounded by dense material produced by strong winds of mass loss rates $\dot{m}_w = 10^{-5} \dot{m}_{w,-5}$ and velocity $v_w = 10^7 v_{w,7}$. This wind scatters back a fraction of the photons produced by the bursts and its afterglow (Thompson & Madau 2000). Doing so, the wind is also accelerated and, when it reaches relativistic velocities, the scattering efficiency decreases. Thus assume that each electron (and the associated proton) scatters photons only until it reaches $\Gamma = 2$, i.e. until it has scattered a total energy of $m_p c^2$ (i.e. $\sim 2,000$ photons of 0.5 MeV each). In this case the back–scattered luminosity L_{back} is constant, since there are an equal number of electrons in a shell of constant width ΔR (for a density profile $\propto R^{-2}$). This luminosity is of the order:

$$L_{\text{back}} \sim m_p c^2 \frac{\dot{m}_w}{m_p v_w / c} = 1.8 \times 10^{45} \frac{\dot{m}_{w,-5}}{v_{w,7}} \text{ erg s}^{-1}. \quad (6)$$

Scattered photons will illuminate the expanding equatorial matter after a time $2R/c$, giving rise to X–ray line emission. At this (short) time, the line would be mainly be produced by K α emission from H–like ^{56}Ni at 8.1 keV. Even if the large expanding velocity makes the transverse Doppler shift important, we require a fine tuned velocity to redshift the 8.1 keV ^{56}Ni line into 6.97 keV. For this reason we consider this scenario unlikely.

4. CONCLUSIONS

The recently detected features in the X–ray afterglow of GRBs give us important information on the nature of the GRB progenitor by imposing significant constraints on models, the most severe being how to arrange a large amount of line emitting material close to the GRB site, while avoiding at the same time a large Thomson scattering opacity. This limit applies to all bursts showing a line feature. A further limit comes from the *Chandra* observation of a *broad* line in GRB 991216. Furthermore, these observations require a very large amount of iron (Eq. 4), such as is known to be contained only in SNe.

In this *Letter* we have presented three models aimed at explaining the observed data: two of them (the “back of the remnant” and “back illuminated equatorial material” models) require that the observed emission line is produced by redshifted

cobalt or nickel (instead of iron), and require some fine tuning and/or ad hoc assumptions. The “wide funnel” model, instead, is in better agreement with observations: its geometry solves the size problem, and the acceleration of the line emitting material by grazing incident photons solves the kinematic problem, allowing the remnant to be a few months old (and allowing enough time for cobalt to decay into iron). This model implies that the GRB progenitors are massive stars exploded as supernovae some months before the burst, populating the vicinity of the burst with iron rich material. This two-step process, and the time-delay between the two steps, are exactly what is predicted in the SupraNova scenario of Vietri & Stella (1998).

Future observations by *BeppoSAX*, *ASCA* and, especially, *Chandra* and *XMM-Newton* (and future missions, such as *Swift* and *Constellation-X*) will address important issues such as the presence of cobalt and nickel lines in the spectrum, revealing the age of the remnant, the line profile, fixing the geometry and kinematics of the emitting region, the possible presence of more than one line, revealing the ionization state, the time evolution of the line and edges, indicative of the characteristics of the illuminator. Together, this information will likely determine whether the line emitting material originates in a “normal”, albeit rare, supernova remnant or if a more exotic explosive phenomenon is required.

REFERENCES

Amati L., et al., 2000, *Science*, 290, 953
 Antonelli A. et al., 2000, *ApJ*, in press (astro-ph/0010221)
 Böttcher M., 2000, *ApJ*, 539, 102
 Filippenko, A.V., et al., 1992, *ApJ*, 384, L15
 Lazzati D., Campana S. & Ghisellini G., 1999, *MNRAS*, 304, L31.
 Piro L., et al., 1999, *ApJ*, 514, L73.
 Piro L., et al., 2000, *Science*, 290, 955 (P2000)
 Pozdnyakov L.A., Sobol I.M. & Sunyaev R.A., 1983, *Astroph. Space Phys. Rev.*, Vol 2, p. 189
 Sollerman J., Kozma C., Fransson C., Leibundgut B., Lundqvist P., Ryde F. & Woudt P., 2000, *ApJ*, 537, L127
 Thompson C. & Madau P., 2000, *ApJ*, 538, 105
 Verner D.A. & Ferland G.J., 1996, *ApJS*, 103, 467
 Vietri M. & Stella L., 1998, *Ap.J.Lett.*, 507, L45.
 Vreeswijk P.M., et al., 2000, *GCN circular* n. 496.
 Yoshida, A., et al., 1999, *Astr. Ap. Suppl.*, 138, 433.
 Weth C., Meszaros P., Kallman T. & Rees M.J., 2000, *ApJ*, 534, 581

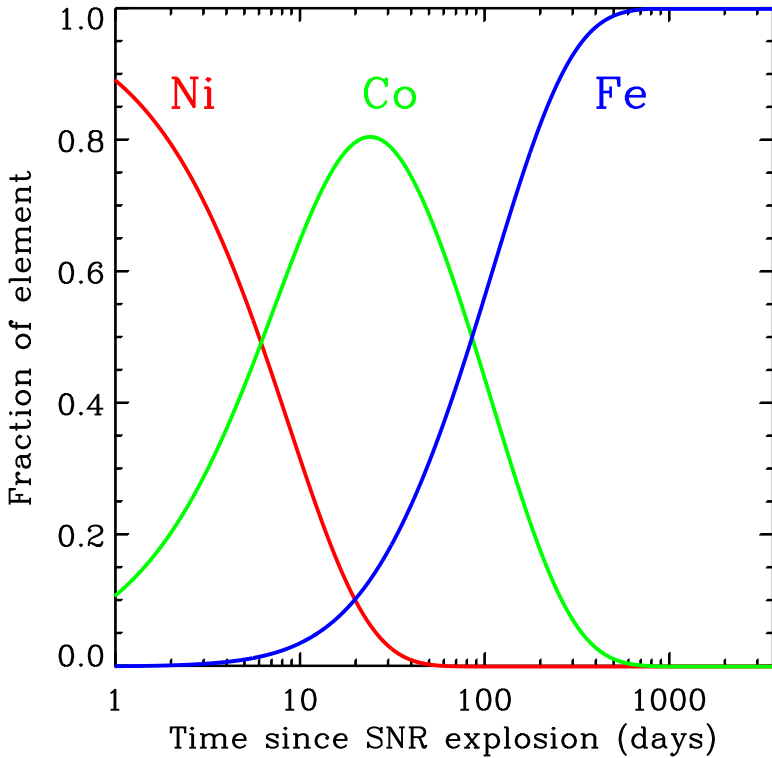


Fig. 1.— The normalized abundances of ^{56}Ni , ^{56}Co and ^{56}Fe as a function of time from the creation of ^{56}Ni . The neutral, He-like, H-like and recombination edge energies are (in keV): ^{56}Ni : 7.478, 7.806, 8.102, 10.775; ^{56}Co : 6.930, 7.242, 7.526, 10.012; ^{56}Fe : 6.404, 6.701, 6.973, 9.278.

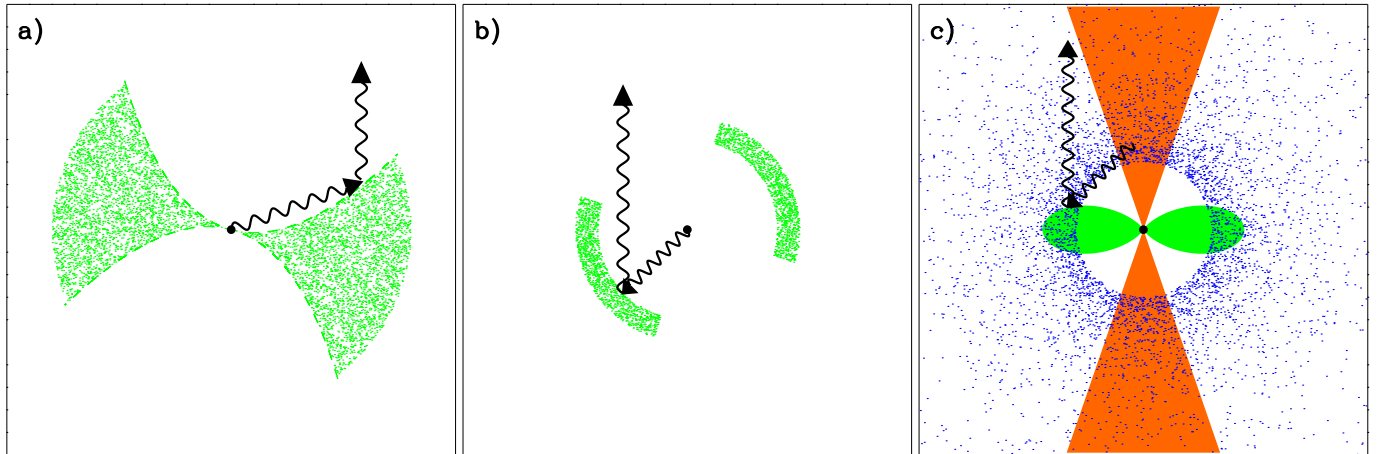


Fig. 2.— Cartoon of the three models discussed in this paper. In panel a) a funnel excavated in a supernova remnant produces the iron line in reflection, by material accelerated to $\sim 10,000 \text{ km s}^{-1}$ by the strong radiation pressure. In panel b) we see the internal parts of a young and receding supernova remnant, in panel c) some equatorial material exploding simultaneously with the burst is illuminated by burst and afterglow photons scattered by the pre-burst stellar wind.